ABSTRACT NO. ISPS2013-2938
ASME Information Storage and Processing Systems Conference, 2013
June 24-25, 2013, Santa Clara, CA, USA

DUAL-STAGE SERVO CONTROL FOR AN OPTICAL POINTING SYSTEM

Eric D. Miller[1*], Raymond A. de Callafon[2]

University of California San Diego
Dept. of Mechanical and Aerospace Engineering, La Jolla, USA
[1]er.dou.mi@gmail.com, [2]callafon@ucsd.edu

1. Introduction

In the realm of hard disk drives (HDD), dual-stage servo control has been shown to achieve increased control bandwidth and reduced power consumption compared to single-stage architectures [1]-[4]. Motivated by these results, we seek to apply dual-stage control to an analogous case of an optical pointing system, which has similar objectives of high-bandwidth control over a wide spatial range.

The particular optical system considered herein consists of a fixed detector, a fast-steering mirror, (FSM), and a two-axis gimbaled mirror called a heliostat (Fig. 1). Due to the conjugate nature of the optics involved, we may equivalently consider the detector as a fixed light source, e.g., a collimated laser beam, which is reflected by the local rotating mirrors toward the remote target. The control objective of this system is to articulate and stabilize the line of sight (LOS) onto the target, in spite of disturbances such as local system vibration and remote target motion.

The key distinction of this optical pointing system in contrast to the HDD is that the final measured output is not a simple linear sum of the two actuator outputs. Instead, the final output depends on the nonlinear, coupled kinematics involved with reflection and rotation of the two mirrors. Furthermore, the optical pointing system is multivariable in nature, with coupling between the two spatial variables as well.

We address these challenges by introducing an inverse-kinematic aspect to the dual-stage controller (K^{-1} in Fig. 2), which masks the open-loop system as a pair of linear MIMO plants. From there, the task of dual-stage controller design can be performed by adapting existing methods developed for HDDs (e.g., the PQ method, as in [2]).

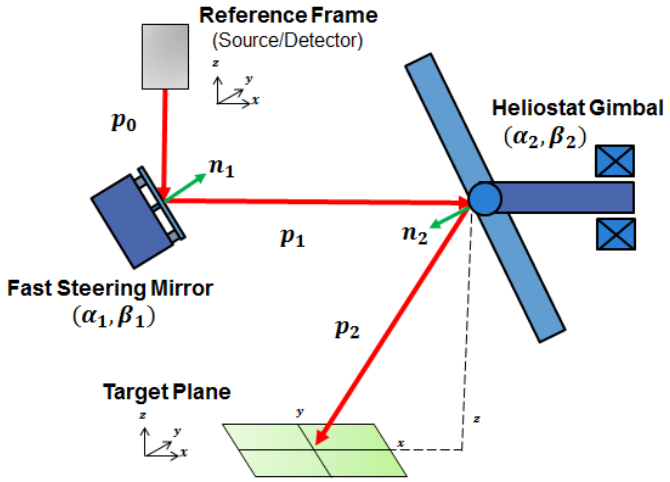

Figure 1. Dual-Stage Mirror-Stabilized Optical Pointing System

An analytical model will be derived, following examples in [8] and [9]. Control system performance will be compared with a single-stage classical controller as a baseline. Simulation will be performed in Simulink.

2. Light Kinematics

We start by deriving a kinematic model to describe the redirection of light through the system as it is reflected by the two rotating mirrors. We define a fixed local coordinate system, centered on the detector, and assume the centers of the two rotating mirrors are fixed in translation to this coordinate system. Next we trace a nominal ray from the detector to the FSM, and describe this ray as a unit vector (p_0) in the local coordinate system. At the FSM, this incident ray is reflected toward the heliostat mirror, where it is reflected again toward the target. Each reflection is modeled as a transformation on the respective incident ray.

$$p_1 = M_1 p_0, \quad p_2 = M_2 p_1 \tag{1}$$

*Corresponding author: Eric D. Miller

The reflection matrices (M_1, M_2) depend on the current orientations of the mirror planes, which are described by unit vector normals in 3-space (n_1, n_2) via the relation

$$M_1 = I_3 - 2n_1 n_1^T, \quad M_2 = I_3 - 2n_2 n_i^T \qquad (2)$$

These mirror plane normal are constructed by rotating the nominal mirror plane normal (n_{10}, n_{20}) by the rotation angles of the mirror joints (3). Rotation matrices R_1 and R_2 will be explained in Section 3 below.

$$n_1 = R_1 n_{10}, \quad n_2 = R_2 n_{20} \qquad (3)$$

Equations (1) through (3) can be combined to yield the output line-of-sight vector,

$$p_2 = [I - 2R_2 n_{02} n_{02}^T R_2^T][I - 2R_1 n_{01} n_{01}^T R_1^T] p_0 \qquad (4)$$

Finally, the measured output variable is the output line-of-sight intersection with the target plane, which we assume is located far below the local platform by a known (i.e., measurable) height z. (We could alternatively assume knowledge of a slant range distance instead; calculating z from this slant range is a simple matter of trigonometry.) The evaluation of this output position (r) is represented by the T block:

$$r = \left(\frac{p_{2x}}{p_{2z}} z \quad \frac{p_{2y}}{p_{2z}} z\right)^T \qquad (5)$$

Finally, the dynamics associated with the mirror actuators and rotational inertias are represented by the two mirror plants P_1 and P_2 (as discussed in the next section), and the complete open-loop model as described so far is illustrated in Fig. 2.

3. Plant Dynamics

The FSM hardware consists of a small flat mirror suspended by flexure mounts, whose orientation is actuated by two pairs of linear-displacement voice-coil actuators (Fig. 3a). The dynamics involved with this mechanism (P_1) can be simply represented by a pair of decoupled second-order spring-mass system transfer functions, as in [13]-[16]. The outputs of this dynamic model are the rotational displacements about the FSM tip/tilt axes (α_1 and β_1), which we multiplex as q_1.

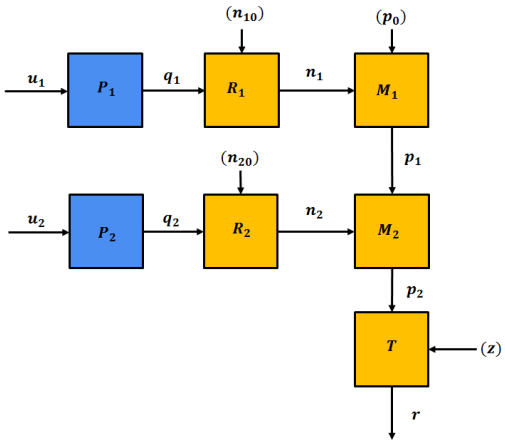

Figure 2. Open-Loop Kinematic/Dynamic Model

For small angles (i.e., where a FSM would be used), cross-coupling between rotation axes can be neglected. Rotations can be combined into a single rotation matrix R_1 which will yield the FSM normal vector n_1.

$$R_1 = \begin{bmatrix} \cos\alpha_1 \cos\beta_1 & \cos\alpha_1 \sin\beta_1 & -\sin\alpha_1 \\ -\sin\beta_1 & \cos\beta_1 & 0 \\ \sin\alpha_1 \cos\beta_1 & \sin\alpha_1 \sin\beta_1 & \cos\alpha_1 \end{bmatrix} \qquad (6)$$

The heliostat features a large flat mirror, gimbaled to rotate about two orthogonal axes, which is also actuated by voice coils. In this case, due to the large range of rotation angles, cross-coupling is present in position and velocity, and a more detailed dynamic model is necessary. Fortunately, ample suitable derivations exist, such as [18] and [19] via Lagrange analysis.

The heliostat dynamic plant (P_2) outputs will be the joint angles of the two rotation axes (α_2 and β_2), and the combined (coupled!) effect of these two rotations on the mirror plant normal is

$$R_2 = \begin{bmatrix} \cos\alpha_2 & 0 & \sin\alpha_2 \\ \sin\beta_2 \sin\alpha_2 & \cos\beta_2 & -\sin\beta_2 \cos\alpha_2 \\ \cos\beta_2 \sin\alpha_2 & \sin\beta_2 & \cos\beta_2 \cos\alpha_2 \end{bmatrix}. \qquad (7)$$

4. Feedback Control Architecture

We consider a system application which is able to measure the final output LOS position on the target plane, with absolute knowledge of the local platform location and attitude relative to the target plane. The control objective will be to stabilize the error between this measured position (r) and the reference position (r^*).

The control architecture will be split into two parts. First, we will use our knowledge about the light kinematics to back out the effective joint angles ($\hat{q}_1$,$\hat{q}_2$), which may be different than the actual joint angles depending on unmodeled kinematic disturbances. Presuming that the light kinematics are nonlinear, we invert the reference position r^* separately from r, and we construct the joint angle error after the inverse kinematic steps. Next, we will design a dual-stage set of MIMO controllers that will drive the joint angle errors to zero. This control architecture is illustrated in Figure 3.

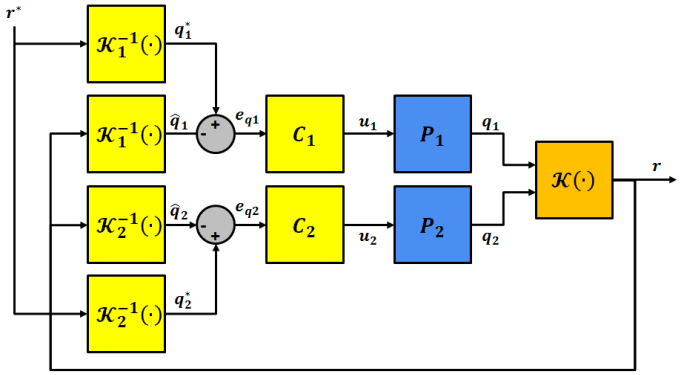

Figure 3. Inverse-Kinematic Dual Stage Control Architecture

5. Inverse Kinematics

In this section we will define the structure of blocks $\mathcal{K}_1^{-1}$ and $\mathcal{K}_2^{-1}$ above. Working from the bottom up in Fig. 2, the effective LOS vector $\tilde{p}_2$ can be easily constructed by normalizing the combination of r and z.

$$p_2 = \frac{[r_x \quad r_y \quad z]}{\|[r_x \quad r_y \quad z]\|_2} \tag{8}$$

The next step is complicated by the indeterminacy in how the two actuator effects combine at the second mirror reflection (block M_2 in Fig 2). Knowing vector $\tilde{p}_2$ alone is not enough to recover the actual positions of the two mirrors. To address this issue, we consider a system with intermediate position feedback measurements available for both mirror mechanisms[1].

Working toward P_2, we use the forward kinematic relations described in Section 2 to get p_1, then we can easily get n_2 via (9).

$$n_2 = \frac{p_2 - p_1}{2} + p_1. \tag{9}$$

From this point, α_2 can be determined by projecting both n_{10} and n_1 onto the yz plane and taking the inverse cosine of the inner product of these projections. Then we can get β_2 by taking the inverse cosine of the inner product of n_{10} and the vector n_1 rotated by α_2.

Now working from M_2 toward P_1, n_2 can be determined using forward kinematic relations on the intermediate feedback of q_2. Knowing n_2, we can get p_1 by pre-multiplying by the inverse of M_2 (which always exists). Joint angles α_1 and β_1 can be determined by the same approach as above.

The desired target plane position r^* can be fed through the forward kinematic models from Section 3 to get the desired effective joint angles q_1^* and q_2^*. In the next section, we will design controllers C_1 and C_2 that will track $\hat{q}_1$ and $\hat{q}_2$ to follow q_1^* and q_2^*.

6. Dual-Stage MIMO Control

The remaining task is to design C_1 and C_2 that will drive the joint angle errors to zero, and to do so in a way that separates the control bandwidths to take advantage of the benefits of dual-stage control.

References

[1] Boettcher, U., de Callafon, R. A., and Talke, F. E., 2010, "Modeling and Control of a Dual Stage Actuator Hard Disk Drive," *Journal of Advanced Mechanical Design, Systems, and Manufacturing, Vol. 4, No. 1.*

[2] Graham, M., Oosterbosch, R.J.M., and de Callafon, R. A., 2005, "Fixed Order PQ-Control Design Method for Dual-Stage Instrumented Suspension," *IEEE Transactions on Magnetics, Vol. 39, No. 5.*

[3] Boettcher, U., Raeymaekers, B., de Callafon, R., A., and Talke, F., E., 2008, "Dynamic Modeling and Control of a Piezo-Electric Dual-Stage Tape Servo Actuator," *IEEE Transactions on Magnetics, Vol. 39, No. 5.*

[4] Guo, G., Hao, Q., and Low, T., 2001, "A Dual-Stage Control Design for High Track per Inch Hard Disk Drives," *IEEE Transactions on Magnetics, Vol. 37, No. 2.*

[5] Rotunno, M., de Callafon, R. A., and Talke, F. E., 2003, "Comparison and Design of Servo Controllers for Dual_Stage Actuators in Hard Disk Drives," *IEEE Transactions on Magnetics, Vol. 39, No. 5.*

[6] Schroek, S. J. and Messner, W. C., 1999, "On Controller Design for Linear Time-Invariant Dual-Input Single-Output Systems," *Proc. of the American Control Conf., Vol 5430.*

[7] de Callafon, R. A., Nagamune, R., and Horowitz, R., 2006, "Robust Dynamic Modeling and Control of Dual-Stage Actuators," *IEEE Transactions on Magnetics, Vol. 42, No. 2.*

[1] In a practical sense, this assumption requires that the FSM and gimbal are equipped with rotary encoders or linear displacement sensors – a configuration which is not uncommon in practice.

[8] DeBruin, J. C., 1991, "Derivation of line-of-sight stabilization equations for gimbaled-mirror optical systems," *Proc. of SPIE, Vol. 1543.*

[9] Royalty, J., 1990, "Development of kinematics for gimbaled mirror sytsems," *Proc. of SPIE, Vol. 1304.*

[10] Hilkert, J. M., 2004, "A comparison of inertial line-of-sight stabilization techniques using mirrors," *Proc. of SPIE, Vol. 5430*.

[11] Hilkert, J. M., 2005, "Kinematic Algorithms for Line-of-Sight Pointing and Scanning using INS / GPS Position and Velocity Information," *Proc. of SPIE, Vol. 5810*.

[12] Hilkert, J. M., 2008, "Inertially Stabilized Platform Technology: Concepts and principles," *IEEE Control Systems Magazine, Vol. 28, No. 1, 26-46.*

[13] Cochran R. W. and Vassar, R. H., 1990, "Fast Steering Mirrors in Optical Control Systems," *SPIE Vol. 1303.*

[14] Zhou, Q., Pinhas, B., Fan, D., and Goldenbergm A. A., 2008, "Design of Fast Steering Mirror Systems for Precision Laser Beams Steering," *IEEE Robotic and Sensors Environments (ROSE), 2008.*

[15] Skormin, V. A., Busch, T. E., and Givens, M. A., 1995, "Model Reference Control of a Fast Steering Mirror of a Pointing, Acquisition and Tracking System for Laser Communications," *Proc. IEEE National Aerospace and Electronics Conference (NAECON) 1995.*

[16] Xie, M., Ma, J., Fu, C., 2000, "Design and experiment of a LQ controller used in high-bandwidth fast steering mirror system," *SPIE Vol. 4025.*

[17] Zhao, Z. M., Yuan, X. Y., Guo, Y., Xu, F., and Li, Z. G., 2010, "Modelling and simulation of a two-axis tracking system," *Journal of Systems and Control Engineering, Vol 224., No 125.*

[18] Skoglar, P., 2002, *Modelling and control of IR/EO-gimbal for UAV surveillance applications,* Master's Thesis, Linköping University, Linköping, Sweden.

[19] Singh, R., Hanmandlu, M., Khatoon, S., and Madsu, V. K., 2008, "Modeling and Simulation of the Dynamics of a Large Size Stabilized Gimbal Platform Assembly," *Asian International Journal of Science and Technology in Production and Manufacturing.*